PAPR Reduction in OFDM Systems: Polynomial-Based Compressing and Iterative Expanding

Mohammad Javad Omidi, Arin Minasian, Hamid Saeedi-Sourck, Keyvan Kasiri & Iraj Hosseini

Wireless Personal Communications
An International Journal

ISSN 0929-6212
Volume 75
Number 1

Wireless Pers Commun (2014)
75:103-118
DOI 10.1007/s11277-013-1350-2

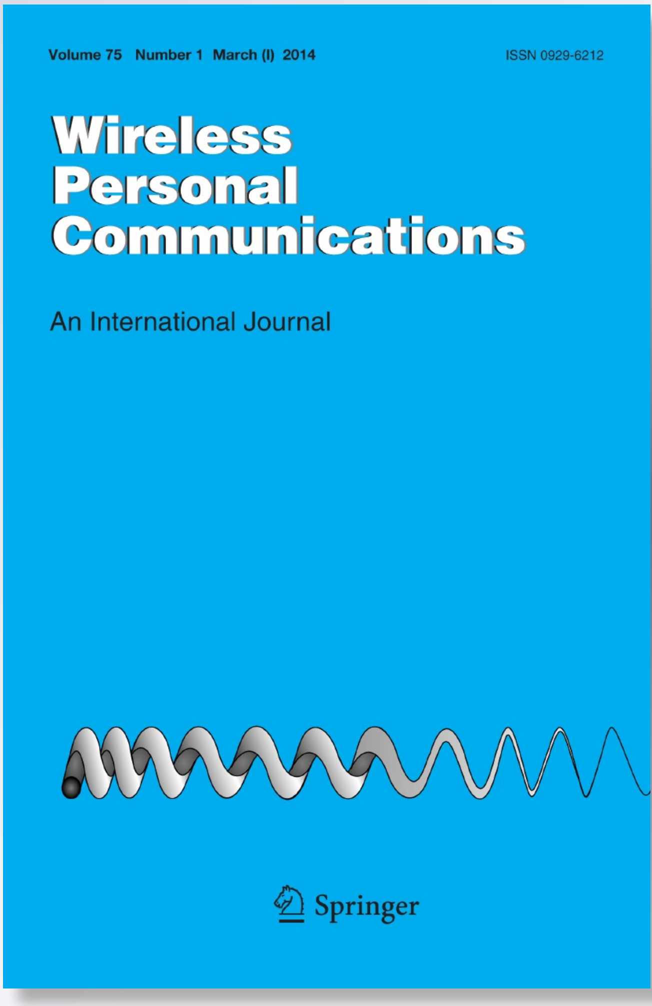

Springer

Wireless Pers Commun (2014) 75:103–118
DOI 10.1007/s11277-013-1350-2

PAPR Reduction in OFDM Systems: Polynomial-Based Compressing and Iterative Expanding

Mohammad Javad Omidi · Arin Minasian · Hamid Saeedi-Sourck · Keyvan Kasiri · Iraj Hosseini

Published online: 21 August 2013

Abstract In this paper a companding-based scheme is proposed to reduce the Peak-to-average power ratio (PAPR) of an orthogonal frequency division multiplexing system. At the transmitter side, a compressing polynomial function is appended to the inverse discrete Fourier transform block; and at the receiver the transmitted signal is retrieved iteratively through combining the discrete Fourier transform block with a reverse expanding function. In the iterative algorithm the Jacobi's method is used for solving the equations. Also, the general form of the compressing polynomial functions is attained through the use of Daubechies wavelet functions. As an advantage, the proposed method involves less complexity at the transmitter compared to other PAPR reduction methods. Furthermore, it requires less increasing to signal-to-noise ratio for the same bit error rate in comparison with other companding methods. The order of compressing polynomial and the number of iterations for the proposed algorithm at the receiver can be set in accordance with the performance-complexity trade off.

M. J. Omidi (✉)
Isfahan University of Technology, Isfahan, Iran
e-mail: omidi@cc.iut.ac.ir

A. Minasian
University of Toronto, Toronto, Canada
e-mail: aminasian@comm.utoronto.ca

H. Saeedi-Sourck
Yazd University, Yazd, Iran
e-mail: saeedi@yazd.ac.ir

K. Kasiri
University of Waterloo, Waterloo, Canada
e-mail: kkasiri@uwaterloo.ca

I. Hosseini
Johns Hopkins University, Baltimore, MD, USA
e-mail: iraj@jhu.edu

Keywords OFDM · PAPR · Companding method · Expanding · Daubechies wavelet

1 Introduction

Orthogonal frequency division multiplexing (OFDM) signaling has gained considerable interest for high data rate transmission applications, due to its high spectral efficiency and the immunity to frequency selective channels [1]. One major drawback of OFDM is the high peak-to-average power ratio (PAPR) of the output signal [2]. Transmitting a signal with high PAPR requires highly linear power amplifiers with a large back-off to avoid adjacent channel interference due to nonlinear effects [3]. Also high values of PAPR result in low efficient usage of the ADC and DAC word length at the analog front ends (AFE) of the transceiver [3]. With a limited number of ADC/DAC bits the designer has to decide about clipping the peaks, which has a deteriorating effect on OFDM signals, or burying the small variations of the signal in the quantization noise. Therefore, dynamic range reduction plays an important role for the application of OFDM signals in both power and band-limited communication systems. Many PAPR reduction techniques have been proposed in the literature, each with certain advantages and disadvantages [2]. These methods can be classified into two categories. The first category of the PAPR reduction schemes, also known as distortion-less techniques, changes the formation of the OFDM signals with high PAPR before multicarrier modulation techniques. Coding techniques use a forward-error-correction code set that excludes the OFDM symbols with a high PAPR, thus reducing the probability of occurrence of a signal with high PAPR [4–6].While these schemes reduce PAPR, they also significantly reduce the transmission rate for OFDM systems with large number of subcarriers [2]. Phase optimization is another distortion-less method that tries to reduce the peaks of the signal by properly rotating the channel constellation. Two phase optimization methods are called the partial transmit sequence (PTS) [7–11] and selective mapping (SLM) [12–14]. These methods have the disadvantages of high computational complexity and side information overhead [2]. In [15] various modifications of the conventional PTS and SLM schemes for achieving a low computational complexity are introduced. Some other proposed methods in this category are tone injection [16,17], tone reservation [18–20], and active constellation extension (ACE) [21,22]. Most of the distortion-less techniques have restrictions on system parameters such as the number of subcarriers, frame format, and constellation type. On the other hand, the signal distortion methods, i.e. the methods that transform the OFDM signals after multicarrier modulation, can be used without restriction on system parameters but at a price of increased bit error rate (BER) [23]. The simplest method in this category is clipping the peak amplitude of the OFDM signal to some desired maximum level; but it is an irreversible nonlinear process that will cause an unacceptable level of noise and out of band distortion in the OFDM signal [24,25]. Although spectrum interference can be reduced by a filter after clipping, the process can cause peak regrowth after D/A conversion [26]. Another effective method in this category is companding. Advantages such as low implementation complexity, good PAPR reduction and BER performance and no bandwidth expansion have made companding one of the most attractive PAPR reduction techniques [2]. Companding can be considered as a type of soft clipping method, in which OFDM signals are companded using a strictly monotonically increasing transform function. Therefore the companded signals can be restored correctly by using the corresponding inverse transform function in the receiver. In [27] the first low-complexity companding technique was proposed by Wang to reduce PAPR. It was based on the speech processing algorithm called μ-law. Using this companding technique small signals are enlarged, while the large signals remain unchanged. However, the average power of input signal is increased that makes companding itself even more sensitive to the nonlinearity of the High Power Amplifier (HPA) [28]. In [29] the authors have provided the design criteria of nonlinear companding transformations to change the distribution of the original OFDM signal into a desirable distribution. They have also proposed novel nonlinear companding transformations that change the distribution of the power or the amplitude of the OFDM signals into uniform distribution. These functions are based on error function. In [30] an exponential companding transform was proposed which transforms the distribution of the amplitude of the original OFDM signals into a uniform distribution. The mentioned companding schemes [29,30] perform better in terms of PAPR reduction and BER performance compared to the μ-law scheme and keep the average power of the signal constant. In [31] two nonlinear companding schemes with iterative receivers were proposed that also outperform the μ-law companding method, however, these methods require additional DFT and IDFT devices. A novel companding method was introduced in [32], which transforms the OFDM signals into trapezium distribution to provide a favorable trade-off between the PAPR reduction and the BER by adjusting two parameters. Since all the companding techniques are sensitive to channel noise, due to the nonlinear processing, more PAPR reduction could lead to lower performance. Therefore, the challenging problem with companding techniques is to reduce PAPR as much as possible while not increasing the BER of the system, out-of-band distortion, and the average power of transmitted signals.

In this paper, a method namely "polynomial-based companding technique" (PCT) is proposed that reduces the PAPR with a polynomial-based compressing function in the transmitter. In addition, using an iterative technique in the receiver results in lower increasing in required SNR for a given BER compared to other companding methods. This method will provide a good tradeoff between the capacity of PAPR reduction, implementation complexity and BER performance by choosing the degree of companding polynomials in the transmitter and the number of iterations for the recovery of original signals at the receiver. Finally the general form of PCT functions is proposed by using Daubechies wavelet functions. As shown in "The Simulation Results Section", the proposed algorithm reduces the PAPR effectively. Also, with higher order polynomials, more reduction can be achieved. Interestingly, there is an inverse relation between the PAPR reduction ability and the BER–SNR performance of proposed method. In other words, system designers can choose an appropriate polynomial order to have a desired performance-complexity trade-off.

The rest of this paper is organized as follows. In Sect. 2, the signal model and the PAPR problem is explained. Section 3 introduces the polynomial-based companding algorithm through a specific set of compressing polynomials at the transmitter and iterative expanding at the receiver. Then, a generalization of polynomial-based functions using well-known Daubechies wavelet functions is proposed. The simulation results and discussions are in Sect. 4. Finally conclusions are drawn in Sect. 5.

2 System Model

A typical OFDM system is presented in Fig. 1. As shown in this figure, the input bit stream is mapped to a constellation space and then the stream of carrier weights $X[k]$, after serial to parallel conversion, is fed to the IDFT block. Let N and $X[k]$, $0 \leq k \leq N-1$, denote

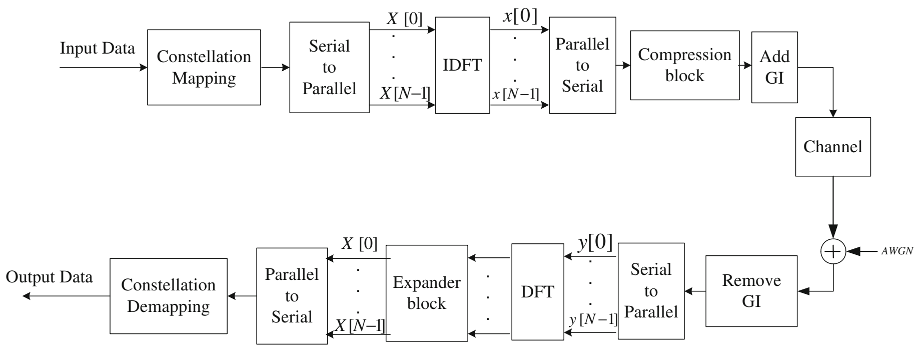

Fig. 1 A typical OFDM system model

the number of subcarriers and the complex modulated symbols in the frequency domain respectively. The output $x[n]$ of the N-point IDFT of $X[k]$ can be mathematically written as

$$x[n] = \frac{1}{N}\sum_{k=0}^{N-1} X[k]e^{j2\pi kn/N}, \quad 0 \le n < N. \tag{1}$$

The PAPR of the transmitted OFDM symbol $x[n]$, $n = 0, 1, \ldots, N-1$, is defined as

$$\text{PAPR}(x[n]) = \frac{\max|x[n]|^2}{E[|x[n]|^2]} \tag{2}$$

where E stands for the expectation operator.

In the proposed method, the resulting time domain signal with high PAPR passes through a compression block which is appended to the IDFT block at the transmitter as shown in Fig. 1. Expansion at the receiver is also performed via an expander block combined with the DFT block.

3 The Proposed Method

In this section, the PCT method is introduced which is based on appending a compressor to the IDFT block at the transmitter and combining an expander with the DFT block at the receiver. In order to reduce the PAPR, compression at the transmitter is performed by scaling the signal based on polynomial functions, which are generalized by means of Daubechies wavelet function. At the other side, the received signal is expanded through an iterative technique following the DFT operation. In the following, we will explain the transmitter and receiver units and the process of obtaining the general form of the polynomial functions in more detail respectively.

3.1 Companding at the Transmitter

In the proposed method, the signal at the transmitter is compressed through a special family of compressing functions. It will be shown that the order of polynomial function can be chosen according to a performance-complexity trade off, see simulation section for more details.

In nonlinear quantization, for a robust performance, SNR of the compressor output should ideally be independent of the probability density function (PDF) of the input. For this reason the compressing function must be logarithmic [33]. However, in an iterative method, the logarithmic function seems not to be proper. Although the μ-law algorithm [27] reduces the PAPR effectively, as it is a logarithmic function, it cannot be employed here as a compander. Hence, the goal is to have low order polynomials as close as possible to the μ-law function.

The compressing function at the transmitter which is applied on a normalized signal is a nonlinear polynomial which reduces the PAPR by increasing the average signal energy while keeping the peak constant. To achieve the required characteristics for the curve, the following restrictions must be applied:

- In order to retrieve the compressed signal at the receiver, the mapping has to be one-to-one and therefore the function must be invertible in the range of [−1,1]. Obviously, it has to be an increasing function to keep the sign of the input data. Thus, its extreme points must not be positioned in this range.
- The polynomial function must have odd symmetry, so it can do identically in both [−1,0] and [0,1]; therefore the terms with even degrees vanish and the origin is the inflection point of the curve.
- Since input data to the block is normalized, the function must take its minimum value at the point (−1,−1) and its maximum value at the point (1,1) in the mentioned range.
- For reducing the PAPR, the data values of low magnitude will be magnified and those of higher magnitude will be kept in a close higher range. Therefore, it is essential to have the lowest slope (ideally zero) at the extreme points and the steepest possible slope at the origin.
- Producing a polynomial function, which is as close as possible to the μ-law compressing function, implies some inflection points in the range of [−1,1]. In our methods we limited the number of inflection points to one in the origin.

Accordingly, the polynomial coefficients are computed. Because of the second requirement, any polynomial function with an odd order satisfies the restrictions. Let us define

$$f(x) = a_p x^p + a_{p-2} x^{p-2} + \cdots + a_5 x^5 + a_3 x^3 + a_1 x \tag{3}$$

where p is an odd number. Coefficients for polynomials of order 3, 5 and 7 are computed as follows

$$\begin{aligned} &p = 3 \Rightarrow a_3 = -1/2, \quad a_1 = 3/2 \\ &p = 5 \Rightarrow a_5 = 3/8, \quad a_3 = -5/4, \quad a_1 = 15/8 \\ &p = 7 \Rightarrow a_7 = -5/16, \quad a_5 = 21/16, \quad a_3 = -35/16, \quad a_1 = 35/16 \end{aligned} \tag{4}$$

Paying attention to a_1, it can be deduced that the higher order polynomials will lead to sharper slopes at the origin. Hence, more reduction in PAPR can be achieved. Due to the lack of known parameters compared to the unknown ones, the coefficients of higher order polynomials cannot be directly calculated in the same manner. In Sect. 3.4, a method is offered to generalize the specified curves for larger p's.

The time domain signal, $x[n] = \{x_0, x_1, \ldots, x_{N-1}\}$, is acquired via IDFT block in (1). To append the polynomial-based compressor to the IDFT, real and imaginary parts of $x[n]$ should be processed separately

$$\Re\{x[n]\} = \frac{1}{N}\sum_{k=0}^{N-1} A_r[n,k] \quad \text{and} \quad \Im\{x[n]\} = \frac{1}{N}\sum_{k=0}^{N-1} A_i[n,k] \tag{5}$$

where

$$\left[A_r[n,k] \; A_i[n,k]\right] = \left[\Re\{X[k]\} \; \Im\{X[k]\}\right]\mathbf{A} \tag{6}$$

and

$$\mathbf{A} = \begin{bmatrix} \cos\left(\frac{2\pi kn}{N}\right) & \sin\left(\frac{2\pi kn}{N}\right) \\ -\sin\left(\frac{2\pi kn}{N}\right) & \cos\left(\frac{2\pi kn}{N}\right) \end{bmatrix} \tag{7}$$

In the conventional companding paradigm, since the complex input to the IDFT has Hermitian symmetry, the output is real. Therefore, compression is applied to the amplitude of the signal. In this paper, because of no symmetry, the real and imaginary parts of the time domain signal should be compressed separately. In order to append the compressing function to the IDFT, polynomials of any order meeting the required conditions can be applied on the sequences $Re\{x[n]\}$ and $Im\{x[n]\}$. Applying the pth order leads to

$$\begin{aligned} \Re\{y[n]\} &= \sum_{j=0}^{\frac{p-1}{2}} a_{(2j+1)} \left(\frac{1}{N} \sum_{k=0}^{N-1} A_r[n,k] \right)^{(2j+1)} \\ \Im\{y[n]\} &= \sum_{j=0}^{\frac{p-1}{2}} a_{(2j+1)} \left(\frac{1}{N} \sum_{k=0}^{N-1} A_i[n,k] \right)^{(2j+1)} \end{aligned} \tag{8}$$

where $y[n]$ represents the compressed signal to be transmitted through the channel.

In the following subsection, an iterative method for the combined expanding/DFT blocks at the receiver is introduced. At first, the method is examined over a noiseless channel, afterwards, it is used for the additive white Gaussian noise (AWGN) one.

3.2 Expanding at the Receiver

At this stage the problem is to find the frequency domain sequence $X[k]$ of length N using the compressed time domain signal $y[n]$ with the same length. As explained in Sect. 3.1, at the transmitter side, $y[n]$ is related to $X[k]$ through a set of nonlinear equations, where n and k meet $0 \le n \le N-1$ and $0 \le k \le N-1$. To solve the set of $2N$ equations with $2N$ known and $2N$ unknown parameters, an iterative method is proposed. By performing adequate number of iterations, the required SNR for a given BER will be lessened compared to non-iterative solution. In this approach, the required number of iterations for given BER and SNR varies with different constellations, DFT sizes and polynomial orders. Due to using an iterative technique, the functions used in the transmitter should be such ones from which the first order of the terms $A_r[n,k]$ and $A_i[n,k]$ and then the unknown values of $\Re\{X[k]\}$ and $\Im\{X[k]\}$ can be derived at any step to enter the next one. Accordingly, using functions such as signum, logarithmic, and exponential, taking absolute values, and using complex magnitudes are not admissible. In this case, polynomial functions seem to be appropriate choices to satisfy the above characteristic and be employed as the compressing function.

Although the relations are nonlinear, each of the unknown values can be derived through the equations. Thus, any linear iterative solution can be exploited. The Jacobi method is the one employed here [34].

For the first iteration, initial values for $X[k]$ are required. As can be seen in Fig. 2, there is a clear resemblance between constellation map of the compressed signal and that of the original signal. So, the DFT of received signal, $y[n]$, can yield a good approximation for $X[k]$. To start each iteration, the terms $A_r^{(m)}[n,k]$ and $A_i^{(m)}[n,k]$ can be obtained at the beginning of the iteration as follows

$$\left[A_r^{(m)}[n,k] \; A_i^{(m)}[n,k] \right] = \left[\Re\{X^{(m)}[k]\} \; \Im\{X^{(m)}[k]\} \right] \mathbf{A} \tag{9}$$

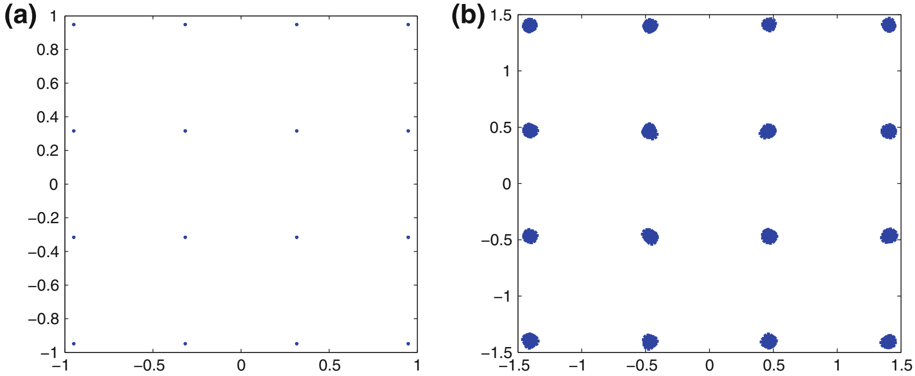

Fig. 2 256 points in 16-QAM constellation. **a** Original signal. **b** Compressed signal

where m represents the iteration number. Then $\hat{x}^{(m)}[n]$, $B_r^m[n,k]$ and $B_i^m[n,k]$ are computed in the following manner. Here, only the real part of equations are considered. Imaginary parts, $\Im\{\hat{x}^{(m)}[n]\}$ and $B_i^m[n,k]$, can be computed in the same manner.

$$\Re\{\hat{x}^{(m)}[n]\} = \sum_{j=0}^{\frac{p-1}{2}} a_{(2j+1)} \left(\frac{1}{N} \sum_{k=0}^{N-1} A_r^{(m)}[n,k] \right)^{(2j+1)} \tag{10}$$

$$B_r^{(m)}[n,k] = \frac{N}{a_1}\left(\Re\{y[n]\} - \left(\Re\{\hat{x}^{(m)}[n]\} - \frac{a_1}{N} A_r^{(m)}[n,k]\right)\right) \tag{11}$$

Next, we compute $\hat{X}^{(m)}[n,k]$ as

$$\left[\Re\{\hat{X}^{(m)}[n,k]\}\ \Im\{\hat{X}^{(m)}[n,k]\}\right] = \left[B_r^{(m)}[n,k]\ B_i^{(m)}[n,k]\right]\mathbf{A}^{-1} \tag{12}$$

Equation (12) shows that for any k, there will be N results for $\Re\{\hat{X}^{(m)}[n,k]\}$ and $\Im\{\hat{X}^{(m)}[n,k]\}$. It is deduced that from the simulation that the average of the N calculated values is the best candidate to replace the previous values of $\Re\{X^{(m)}[k]\}$ and $\Im\{X^{(m)}[k]\}$, or equivalently $X^{(m+1)}[k]$, for the next iteration.

In general, for an ideal channel, after a few iterations, the results will converge to the desired values. However, for low SNR conditions, the obtained values of $(1/N)A_r[n,k]$ and $(1/N)A_i[n,k]$ lie outside the range $[-1,1]$. Since, the extreme points of the polynomials are located at the beginning and end of this range and also our polynomial functions have a high derivative out of the mentioned range, the obtained values beyond $[-1,1]$ will be exposed to the high derivative part of the function. During the next iterations, the results will move farther from the original signal values. Consequently, the values of $\Re\{X[k]\}$ and $\Im\{X[k]\}$ will drastically diverge and thus, the algorithm will ultimately turn towards divergence.

For AWGN channel, to prevent the algorithm from diverging, the out-of-range values of the $(1/N)A_r[n,k]$ and $(1/N)A_i[n,k]$, while keeping their signs, can be substituted for the values of the extreme points. As the simplest but not efficient way, it guarantees the system-convergence. More efficiently, one may suggest using a linear function such as ramp with an arbitrary slope outside the $[-1,1]$ range. It is inferred from the simulation results that its slope could be determined to achieve the best efficiency in terms of system-performance. In other words, for any SNR value, it is possible to choose a proper ramp function with the specified slope, which is able to yield the most accurate converged responses. Using this technique for noisy channels will result in more iterations to converge compared to the noiseless situation.

3.3 Complexity Analysis

At the transmitter, for each symbol in an OFDM block, the proposed method evaluates a polynomial of order p. Therefore, the complexity of this method is $\mathcal{O}(p)$ per symbol or $\mathcal{O}(Np)$ per each OFDM block. The complexity of the companding algorithm is similar to that of other well-known companding schemes introduced in [27,29,30] and [32] since in all of these methods a nonlinear function has to be evaluated for each symbol in the OFDM block. However, our proposed method could be implemented easier since our companding function is a polynomial.

The complexity of expanding algorithm per iterations per block is $\mathcal{O}(N^2 + N^2 p + N^2 + N^3)$. The first N^2 is because in (9) we have to calculate N^2 values by doing a constant size matrix multiplication. Then in (10), for each symbol, the algorithm evaluates a polynomial of order p for given value of $\frac{1}{N}\sum_{k=0}^{N-1} A_r^{(m)}[n,k]$, which requires N calculations on its own. This yields the term $N^2 p$ in the order of complexity. Next in (11) again we have to do N^2 constant time operations. Finally, for each k, we have to calculate $\Re\{\hat{X}^{(m)}[n,k]\}$, $\Im\{\hat{X}^{(m)}[n,k]\}$ for $n = 0, \ldots, N-1$ and then average over them to find the next $X^{(m+1)}[k]$. This results in the term N^3 in the order of complexity. This leads to a more computationally complex algorithm in the receiver compared to other well-known companding schemes in the literature.

3.4 Generalized Compressing Function Using Daubechies Wavelet Functions

Obtaining proposed curves and specifying their characteristics in Sect. 3.1, it can be verified that there exist similarities between companding polynomials and Daubechies wavelet functions [35], but some modifications such as scaling and time shifitng are needed to convert Daubechies functions to the compressing ones.

Daubechies wavelets of general order are defined in the following form:

$$P_k(x) = 2\sum_{n=0}^{k-1}\binom{k+n-1}{n} x^n (1-x)^k \tag{13}$$

while $k = 1, 2, 3, \ldots$ and the order of $P_k(x)$ is denoted through k, such that $O(P_k(x)) = 2k - 1$.

These polynomials have some remarkable properties such as passing smoothly from 2 to 0 (with the exception of $k = 1$), zero slope at both $x = 0$ and $x = 1$ and having a inflection point at (0.5, 1). These properties make this family of curves desirable for deriving companding functions.

In order to obtain the desired compressing functions, it is required to modify Daubechies wavelets. Using a linear transformation of $x = (t + 1)/2$, the general form of compressing functions will be:

$$f(t) = -(P_k(t) - 1) \tag{14}$$

It is clear that $O(f(t)) = 2k - 1$. Finally, the above relation will bring about the result as follows:

$$f_m(t) = 1 - \left(\frac{1}{2}\right)^{\frac{m-1}{2}} (1-t)^{\frac{m+1}{2}} \sum_{n=0}^{\frac{m-1}{2}} \left(\frac{1}{2}\right)^n \binom{\frac{m-1}{2}+n}{n} (t+1)^n \quad \text{where } m = 2k-1 \tag{15}$$

Here m stands for the polynomial order. It is evident that not only (15) covers all the results obtained in Sect. 3.1, for orders 3, 5 and 7, but also polynomials of general order can be simply attained.

4 The Simulation Results

In order to analyze the operation of the system in terms of PAPR reduction and BER performance and their relationship for the proposed algorithm, 10^5 randomly generated data modulated by 64-QAM constellation map and $N = 2,048$ subcarriers is used for PAPR-CCDF and power spectrum density simulations and 64-QAM modulation and $N = 256$ subcarriers were used for BER–SNR performance evaluation. The AWGN channel without channel encoding is employed in our experiments. Also, to evaluate the performance of the proposed method in terms of PAPR reduction and BER–SNR performance, we have compared our results with three other well-known companding methods. These three methods are uniform companding [29], exponential companding [30] and trapezoidal companding [32]. It is worth mentioning that as the methods introduced in [29,30,32] outperform the conventional μ-law companding technique in terms of PAPR reduction and BER-SNR performance, and in order to represent the figures more clearly, we have not included the results associated with μ-law method. The results are presented in following order. First CCDF of the required PAPR is presented. Then the effect of iteration and polynomial order on improving system-performance for different polynomial orders of PCT with a fixed DFT size and constellation is expressed. After that the relation between DFT size and complexity of the receiver in the form of BER–SNR plots is shown. The effect of slope of the ramp function on the system-performance and finally problem of power spectral density (PSD) are also examined.

4.1 CCDF of the Required PAPR

The PAPR-CCDF for the original signal, compressed signals with polynomials of order 3, 7, 11, 25, 37, 55, uniform compressed signal and exponential compressed signal with $d = 2$ and trapezoidal compressed signal with $q = \frac{2}{3}$ with a fixed DFT size ($N = 2,048$) and 64-QAM-constellation is depicted in Fig. 3. According to performance-complexity trade-off, it is not feasible to simulate the higher order polynomials.

As is observed, the algorithm reduces the PAPR of the signal effectively. Also, with higher order polynomials, more reduction can be achieved. As shown in this figure, by choosing a proper polynomial order, this method can outperform the other well known methods in terms of PAPR reduction.

4.2 SNR required for a given BER

Figure 4 illustrates the effect of number of iterations on system-performance where the 7th order polynomial is employed. Since there is no differences between different curves for low SNR values, i.e. less than 10dB, DFT with no iteration can be used. Focusing on the

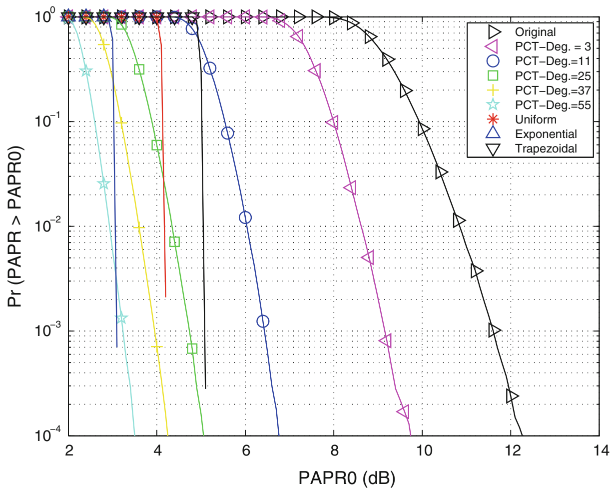

Fig. 3 The CCDF of PAPR for original and compressed signals

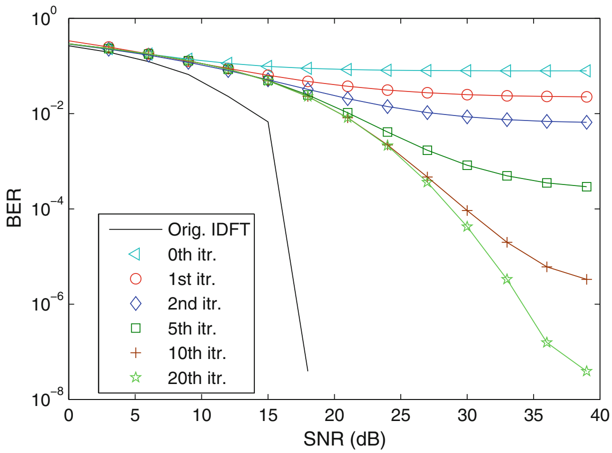

Fig. 4 Effect of iteration on system performance for the 5th order polynomial

negligible differences between iterations more than 5, it is obvious that after a certain number of iterations, the performance cannot improve considerably. We can heuristically define an iteration after which, performance of the system for a given BER and polynomial order will not improve noticeably as a "suitable" iteration. It is not a precise definition, in other words system designers can use their own suitable iteration for a fixed polynomial order in order to have an appropriate performance-complexity trade-off.

Figure 5 shows the effect of different polynomial orders, where "suitable" number of iterations is chosen at the receiver to expand the signals. In this figure the SNR–BER plot for PCT polynomials of order 3, 7, 11 and 25 with 3, 9, 49 and 49 iterations, the original not companded signal, uniform compressed signal, exponential compressed signal with $d = 2$, and trapezoidal compressed signal with $q = \frac{2}{3}$ are depicted. It is concluded that there is an inverse relation between the PAPR reduction ability and the BER–SNR performance of PCT

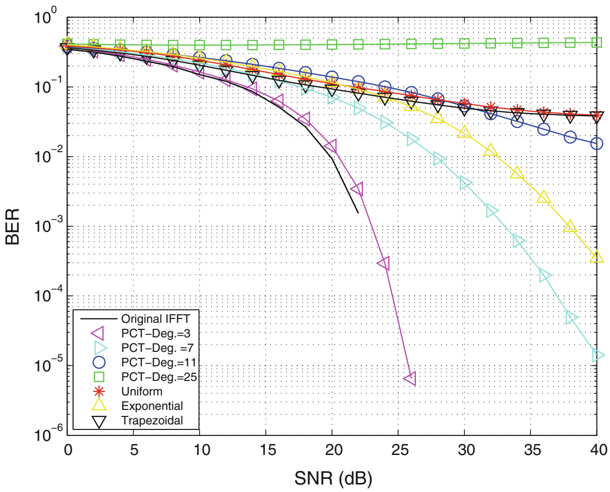

Fig. 5 System performance for original and compressed signals

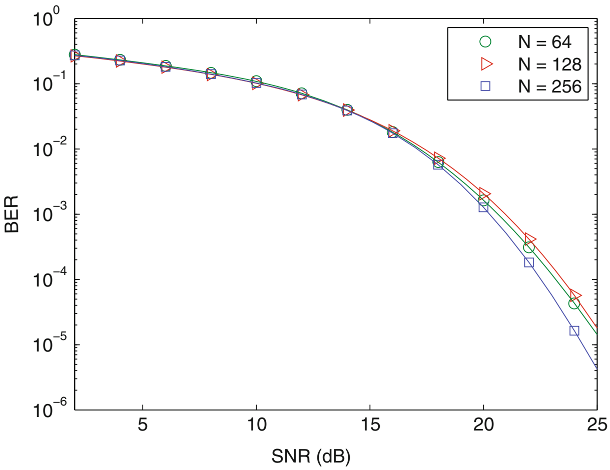

Fig. 6 The system-performance for 16-QAM, 5th order polynomial, 7 iteration and different DFT sizes

signals. As is shown, the 3rd order polynomial outperforms the higher orders of PCT as well as the other companding techniques in terms of BER–SNR performance.

It is apparent that using the constellation with more points increases the SNR of the system for a given BER, however, using this constellation gives us more transmission rate. Nevertheless, what we are concerned about is whether the suitable iteration and consequently computational complexity for the same performance change in the case that we use the same constellation and polynomial order but different DFT sizes.

The system-performance for 16-QAM, 5th order polynomial, 7 iterations and different DFT sizes is shown in Fig. 6. It is understood that under the circumstance of fixed polynomial order, constellation and SNR of the system, the number of iterations needed for the given BER and therefore complexity of the system never increases. For this purpose, SNR–BER plots for the 5th polynomial order, 16-QAM constellation and $N = 64, 128, 256$ and 7 iteration

Table 1 Effect of ramp slope on improving performance of the system

Ramp slope	0	0.25	0.5	1	2	4	6
SNR	25.29	24.19	23.57	23.15	22.93	22.92	22.90

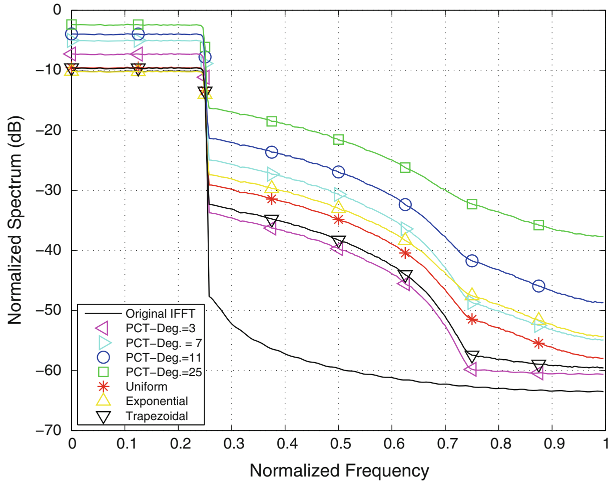

Fig. 7 Power spectrum density of the original and compressed OFDM signals

for each are shown in Fig. 6. It can be seen that, under the same condition of constellation, polynomial order and number of iterations, with the increase in the DFT size from 64 to 256 the performance of the system does not vary considerably. This is a noticeable point that with the large amount of sub-carriers in recent OFDM systems, performance of the system not only never decreases but also it is probable to improve the system-performance with no increase in the complexity of the system.

4.3 Effect of Ramp on the Performance

In order to avoid the system from divergence, a ramp function outside $[-1,1]$ is considered. In this part, effect of the ramp slope on the performance of the system is examined. Table 1 shows the required SNR of the system when BER $= 10^{-4}$ for the 5th order polynomial and 7th iteration. A system designer can omit the effect of ramp slope on the performance, but to optimize the design, the ramp slope should be considered. It should be noted that all the results presented in other parts are obtained through slope 6.

4.4 Power Spectrum Density

Many PAPR reduction schemes cause spectrum side-lobes generation in PSD plot. The spectrum of the uncompressed and compressed OFDM signals by different orders of PCT, uniform, exponential and trapezoidal companding methods are shown in Fig. 7. It can be seen that at the frequency twice the bandwidth of the main lobe,approximately, there is about 60 dB attenuation in the original OFDM spectrum, but this attenuation is about 40 dB for the compressed signal by the 3rd order polynomial. This attenuation decreases as the order of polynomials increases. It is observed that the 3rd order PCT has a better spectrum characteristic and spectral regrowth caused by PAPR reduction compared to the other three methods. In practical systems, the band-pass filter (BPF) is necessary but the BPF by itself causes the degradation of the error rate performance.

5 Conclusion

In this paper, a PAPR reduction technique called PCT was introduced using polynomial-based compressing in the transmitter and an iterative expanding algorithm at the receiver. In addition, the general form of PCT functions was derived by using Daubechies wavelet functions. Results from different simulations showed that increasing the polynomial order reduces the PAPR while decreasing the BER–SNR performance. Running more iterations at the receiver improved the performance in exchange for more computation. In the procedure of designing OFDM systems, the polynomial order and the suitable number of iterations can be selected based on the above results and the specific requirements that the system must meet.

References

1. Wu, Y., & Zou, W. Y. (1999). Orthogonal frequency division multiplexing: A multi-carrier modulation scheme. *IEEE Transaction on Consumer Electronics*, *41*(3), 392–399.
2. Jiang, T., & Wu, Y. (2008). An overview: Peak-to-average power ratio reduction techniques for OFDM signals. *IEEE Transaction on Broadcasting*, *54*(2), 257–268.
3. Conti, A., Dardari, D., & Tralli, V. (2000). On the performance of CDMA systems with nonlinear amplifier and AWGN. In *Proceeding of 6th IEEE international symposium on spread spectrum techniques and applications* (pp. 197–202). New Jersey, USA.
4. Jones, A. E., Wilkinson, T. A., & Barton, S. (1994). Block coding scheme for reduction of peak to mean envelope power ratio of multicarrier transmission schemes. *IEE Electronics Letters*, *30*(25), 2098–2099.
5. Jiang, T., & Zhu, G. (2005). Complement block coding for reduction in peak-to-average power ratio of OFDM signals. *IEEE Communications Magazine*, *43*(9), S17–S22.
6. van Nee, R. D. J. (1996). OFDM codes for peak-to-average power reduction and error correction. *Global Telecommunications Conference,* pp. 740–744.
7. Cimini, L. J, Jr, & Sollenberger, N. R. (2000). Peak-to-average power ratio reduction of an OFDM signal using partial transmit sequences. *IEEE Communication Letters*, *4*(3), 86–88.
8. Muller, S. H., & Hüber, J. B. (1997). OFDM with reduced peak-to-average power ratio by optimum combination of partial transmit sequences. *IEE Electronic Letter*, *33*(5), 368–369.
9. Ho, W. S., Madhukumar, W. S., & Chin, F. (2003). Peak-to-average power reduction using partial transmit sequences: A suboptimal approach based on dual layered phase sequencing. *IEEE Transaction on Broadcasting*, *49*(2), 225–231.
10. Kang, S. G., Kim, J. G., & Joo, E. K. (1999). A novel subblock partition scheme for partial transmit sequence OFDM. *IEEE Transaction on Broadcasting*, *45*(3), 333–338.
11. Kwon, O. J., & Ha, Y. H. (2003). Multi-carrier PAP reduction method using sub-optimal PTS with threshold. *IEEE Transaction on Broadcasting*, *49*(2), 232–236.
12. Breiling, M., Muller-Weinfurtner, S. H., & Huber, J. B. (2003). SLM peak-power reduction without explicit side information. *IEEE Communalization Letters*, *5*(6), 239–241.
13. Bami, R. W., Fischer, R. F. H., & Hüber, J. B. (1996). Reducing the peak-to-average power ratio of multicarrier modulation by selective mapping. *IEE Electronic Letter*, *32*(22), 2056–2057.
14. Han, S. H., & Lee, J. H. (2004). Modified selected mapping technique for PAPR reduction of coded OFDM signal. *IEEE Transaction on Broadcasting*, *50*(3), 335–341.
15. Lim, D. W., Heo, S. J., & No, J. S. (2009). An overview of peak-to-average power ratio reduction schemes for OFDM signals. *Journal of Communications and Networks*, *11*(3), 229–239.
16. Tellado, J. (2000). *Multicarrier modulation with low PAPR: Applications to DSL and wireless*. Berlin: Kluwer.
17. Tellado, J., & Ciofi, J. M. (1998). PAPR reduction with minimal or zero bandwidth loss and low complexity. ANSI document, T1E1.4, pp. 98–173.

18. Gatherer, A., & Polley, M. (1997). Controlling clipping probability in DMT transmission. *Proceeding of IEEE Asilomar conference*, *1*, 578–584.
19. Petersson, N., Johansson, A., Odling, P., & Börjesson, P. O. (2001). Analysis of tone selection for PAPR reduction. In *Proceeding international conference on information, communications and signal processing*, Singapore.
20. Borjesson, P. O., Feichtinger, H. G., Grip, N., Isaksson M., Kaiblinger, N., Odling, P., & Persson, L. E. (1999). A low-complexity PAPR-reduction method for DMT-VDSL. In *Proceeding of the 5th international symposium on digital signal processing for communication systems*, Australia, pp. 164–199.
21. Jones, D. L. (1999). Peak power reduction in OFDM and DMT via active channel modification. In *Proceeding of IEEE Asilomar conference on signals, systems, and computers*, pp. 1076–1079.
22. Krongold, B. S., & Jones, D. L. (2002). A study of active constellation extension for PAPR reduction in OFDM. In *Proceeding international OFDM workshop*, pp. 107–111, Germany.
23. Aburakhia, S. A., Badran, E. F., & Mohamed, D. A. E. (2009). Linear companding transform for the reduction of peak-to-average power ratio of OFDM signals. *IEEE Transaction on Broadcasting*, *55*(1), 155–160.
24. Li, X., & Cimini, L. J, Jr. (1998). Effects of clipping and filtering on the performance of OFDM. *IEEE Communication Letters*, *2*(5), 131–133.
25. Armstrong, J. (2002). Peak-to-average power reduction for OFDM by repeated clipping and frequency domain filtering. *Electronics Letters*, *38*(5), 246–247.
26. Ochiai, H., & Imai, H. (2000). Performance of the deliberate clipping with adaptive symbol selection for strictly band-limited OFDM systems. *IEEE Journal on Selected Areas in Communication*, *18*(11), 2270–2277.
27. Wang, X., Tjhung, T. T., & Ng, C. S. (1999). Reduction of peak-to-average power ratio of OFDM system using a companding technique. *IEEE Transaction on Broadcastaing*, *45*(3), 303–307.
28. Matsson, Anders, Mendenhall, Geoffrey, & Dittmer Harris, T. (1999). Comments on: Reduction of peak-to average power ratio of OFDM system using a companding technique. *IEEE Transaction on Broadcasting*, *45*(4), 418–419.
29. Jaing, T., Xiang, W., Richardson, P. C., Qu, D., & Zhu, G. (2007). On the nonlinear companding transform for reduction in PAPR of MCM. *IEEE Transaction on Wireless Communication*, *6*(6), 2017–2021.
30. Jiang, T., Yang, Y., & Song, Y. (2005). Exponential companding transform for PAPR reduction in OFDM systems. *IEEE Transaction on Broadcasting*, *51*(2), 244–248.
31. Jiang, T., Yao, W., Guo, P., Song, Y., & Qu, D. (2006). Two novel nonlinear companding schemes with iterative receiver to reduce PAPR in multi-carrier modulation systems. *IEEE Transaction on Broadcasting*, *52*(2), 268–273.
32. Jeng, S.-S., & Chen, J.-M. (2011). Efficient PAPR reduction in OFDM systems based on a companding technique With trapezium distribution. *IEEE Transaction on Broadcasting*, *57*(2), 291–298.
33. Haykin, S. (1998). *Digital communications* (2nd ed.). New York, USA: Wiley.
34. Barrett, R., Berry, M., Chan, T. F., Demmel, J., Donato, J., Dongarra, J., et al. (1994). *Templates for the solution of linear systems: Building blocks for iterative methods* (2nd ed.). Philadelphia: SIAM.
35. Walnut, D. F. (2003). *An introduction to wavelet analysis (Applied and Numerical Harmonic Analysis), 264–269*. Boston: Birkhäuser.

Author Biographies

Mohammad Javad Omidi received his Ph.D. from University of Toronto in 1998. He has gained years of industry experience in Canada as the cofounder of an active research and development group designing broadband communication systems. He is an Assistant Professor in the Department of Electrical and Computer Engineering, Isfahan University of Technology, Iran, and has been the chair of Information Technology Center (2005–2008), and chair of Electrical and Computer Engineering Department (2008–2011) and manager of Communication Group (2011–) at this university. His research interests are in the areas of Mobile Computing, Wireless Communications, Digital Communication Systems, Software Defined Radio and Cognitive Radio Systems, and VLSI Architectures for Communication Algorithms. He has several publications, US and international patents and inventions on all the areas of his research interest.

Arin Minasian received the B.Sc. degree from the Isfahan University of Technology (IUT), Iran, in 2012 in electrical engineering. He is currently a M.A.Sc. student in University of Toronto, Canada. His research interest include: Wireless communications, energy harvesting communications and information theory.

Hamid Saeedi-Sourck received the B.Sc., M.Sc., and Ph.D. degrees from the Isfahan University of Technology (IUT), Iran, in 2001, 2003, and 2011 respectively, all in electrical engineering. From 2003–2007, he worked as a researcher in the Electrical and Computer Engineering research center of IUT. Currently he is an Assistant Professor in the Department of Electrical and Computer Engineering, Yazd University, Iran. His research interests include: Signal processing for wireless communications, Multi-carrier modulation, Cognitive radios, Radar systems, and Wavelet transform.

Keyvan Kasiri received the B.Sc. degree in Electrical and Computer Engineering (ECE) from the Isfahan University of Technology, Iran, in 2007 and the M.Sc. degree in Electrical Engineering from the Shiraz University of Technology, Shiraz, Iran in 2010. He joined the Vision and Image Processing Research Group, University of Waterloo, Canada, in 2011. Keyvan is currently working towards the Ph.D. degree in the Department of Systems Design Engineering at the University of Waterloo. His research interests include different aspects of signal and image processing, analysis of biomedical images, pattern recognition, and machine learning.

Iraj Hosseini received his B.Sc. in Electrical and Computer Engineering (ECE) from Isfahan University of Technology, Iran in 2007. In 2009, Iraj obtained his M.Sc. in ECE from the University of Alberta (UofA), Canada. At UofA, he received several prestigious awards including the *iCORE Scholarship for International Students* and the *Alberta Ingenuity Graduate Student Scholarship*. Iraj is currently a 5th-year Ph.D. student in the Department of Biomedical Engineering at Johns Hopkins University. At Hopkins, Iraj was awarded the *Ruth H. Aranow Fellowship* in Computational Medicine in 2012.